



PUBLISHED FOR SISSA BY SPRINGER

RECEIVED: May 9, 2011

REVISED: July 15, 2011

ACCEPTED: August 4, 2011

PUBLISHED: August 22, 2011

Probing the supersymmetric type III seesaw: LFV at low-energies and at the LHC

A. Abada,^a A.J.R. Figueiredo,^b J.C. Romão^b and A.M. Teixeira^c

^a*Laboratoire de Physique Théorique, CNRS — UMR 8627,
Université de Paris-Sud 1, F-91405 Orsay Cedex, France*

^b*Centro de Física Teórica de Partículas, Instituto Superior Técnico,
Av. Rovisco Pais 1, 1049-001 Lisboa, Portugal*

^c*Laboratoire de Physique Corpusculaire, CNRS/IN2P3 — UMR 6533,
Campus des Cézeaux, 24 Av. des Landais, F-63171 Aubière Cedex, France*

E-mail: abada@th.u-psud.fr, ajrf@cftp.ist.utl.pt,
jorge.romao@ist.utl.pt, ana.teixeira@clermont.in2p3.fr

ABSTRACT: We consider a supersymmetric type III seesaw, where the additional heavy states are embedded into complete SU(5) representations to preserve gauge coupling unification. Complying with phenomenological and experimental constraints strongly tightens the viable parameter space of the model. In particular, one expects very characteristic signals of lepton flavour violation both at low-energies and at the LHC, which offer the possibility of falsifying the model.

KEYWORDS: Neutrino Physics, Supersymmetric Standard Model

ARXIV EPRINT: [1104.3962v1](https://arxiv.org/abs/1104.3962v1)

Contents

1	Introduction	1
2	Type III SUSY seesaw	3
3	Lepton flavour violation in a type III SUSY seesaw	5
4	Numerical results and discussion	9
5	Conclusions	19

1 Introduction

The seesaw mechanism, in its different realisations, constitutes one of the simplest and yet most elegant ways to explain neutrino masses and mixings. In the minimal realisations of the seesaw, the Standard Model (SM) can be extended by the addition of fermionic singlets (type I seesaw) [1–5], scalar triplets (type II) [6–12] or fermionic triplets (type III) [13, 14]. Although dependent on the size of the neutrino Yukawa couplings (Y^ν), these new states are in general heavy: assuming natural couplings, $Y^\nu \sim 1$, their masses can be close to the Grand Unified Theory (GUT) scale, $\mathcal{O}(10^{16} \text{ GeV})$.

If these states are indeed at the origin of neutrino mass generation, it is important to investigate which seesaw realisation (or combination thereof) is at work. Indeed, if the mass of the mediators is such that production at present colliders is possible (in this case $Y^\nu \sim 10^{-6}$), then one can devise strategies for their direct searches. On the contrary, if they are very heavy, then they cannot be directly probed, and their indirect signatures in low-energy observables (typically via higher order corrections) will be extremely suppressed.

Other than the mechanism of neutrino mass generation, there are several reasons — theoretical issues and observational problems — motivating the extension (or embedding) of the SM into a larger framework. Supersymmetry (SUSY) is a well motivated solution for the hierarchy problem that also offers an elegant solution for the non-baryonic dark matter (DM) problem of the Universe [15–17]. If the Large Hadron Collider (LHC) indeed finds signatures of SUSY, it is then extremely appealing to consider the embedding of a seesaw mechanism into a supersymmetric framework (the so-called SUSY seesaw).

Supersymmetric seesaws lead to a number of possible signatures in the neutral and charged lepton sectors, both at low and high energies. Among low-energy observables, the most striking SUSY seesaw impact is perhaps the possibility of having charged lepton flavour violating (LFV) transitions. Indeed, one can have sizable contributions to radiative decays ($\ell_i \rightarrow \ell_j \gamma$), three-body decays ($\ell_i \rightarrow 3 \ell_j$) and $\mu - e$ transitions in heavy nuclei, well within reach of current and/or future dedicated facilities [18–40]. At high-energy colliders,

such as the LHC, several observables may reflect an underlying SUSY seesaw. Let us begin by noticing that if some components of the seesaw mediators are not singlets under the SM gauge group (which is the case in type II and III seesaws), the latter can leave an imprint on the SUSY spectrum, since they can modify the supersymmetric β -functions governing the evolution of the gauge couplings and soft-SUSY breaking parameters. At the LHC, SUSY seesaws can also give rise to several LFV signals: firstly, one can have sizable widths for LFV decay processes like $\chi_2^0 \rightarrow \chi_1^0 \ell_i^\pm \ell_j^\mp$ [38, 41–44]; secondly, one can have observable flavoured slepton mass splittings (MS), $\Delta m_{\tilde{\ell}}/m_{\tilde{\ell}}$ ($\tilde{e}_L, \tilde{\mu}_L$) and possibly $\Delta m_{\tilde{\ell}}/m_{\tilde{\ell}}$ ($\tilde{\mu}_L, \tilde{\tau}_2$). These splittings can be identified since, under certain conditions, one can effectively reconstruct slepton masses via observables such as the kinematic end-point of the invariant mass distribution of the leptons coming from the cascade decays $\chi_2^0 \rightarrow \tilde{\ell}^\pm \ell^\mp \rightarrow \chi_1^0 \ell^\pm \ell^\mp$. If the slepton in the decay chain is real (on-shell), the di-lepton invariant mass spectrum has a kinematical edge that might then be measured with a very high precision (up to 0.1 %) [45–47]. Together with data arising from other observables, this information allows to reconstruct the slepton masses [45–50] and hence study the slepton mass splittings. Finally, one can observe multiple edges in di-lepton invariant mass distributions from $\chi_2^0 \rightarrow \chi_1^0 \ell_i^\pm \ell_i^\mp$, arising from the exchange of a different flavour slepton $\tilde{\ell}_j$ (in addition to the left- and right-handed sleptons, $\tilde{\ell}_{L,R}^i$). Under the assumption of a seesaw as the unique underlying source of flavour violation in the leptonic sector (for instance assuming that SUSY breaking is due to flavour blind interactions), then all the above observables, both at high and low energies, will be strongly correlated.

Each seesaw realisation will have a distinct impact on the latter observables. It is thus mandatory to conduct an exhaustive study of the many possible experimental signatures, in order to test the seesaw hypothesis, either excluding or substantiating it, and in the latter case, devising a strategy to disentangle among the different seesaw realisations.

In a previous work [51] we have studied the impact of a type I seesaw, embedded into the constrained minimal supersymmetric extension of the SM (cMSSM), in what concerns lepton flavour violation both at low-energies and at the LHC. Here we extend the analysis to the type III SUSY seesaw. In this case, and in order to accommodate neutrino masses and mixings, one adds (at least two) fermionic SU(2) triplets to the SM particle field content [52], as well as the corresponding superpartners. If one extends the usual MSSM by just the superfields responsible for neutrino masses and mixings, one would destroy the nice feature of gauge coupling unification. This problem is easily circumvented by embedding the new states in complete SU(5) representations, **24**-plets in the case of a type III seesaw [53]. Note that in addition to the SU(2) triplet, the **24**-plet contains a singlet state which also contributes to neutrino dynamics, so that in this case one actually has a mixture between type I and type III seesaws.

Our study shows that if a type III seesaw is indeed the unique source of neutrino masses and leptonic mixings, and is realised within an otherwise flavour conserving SUSY extension of the SM (specifically the cMSSM), one then expects low-energy LFV observables within future sensitivity reach, as well as interesting slepton phenomena at the LHC. After having identified regions in the cMSSM parameter space, where the slepton masses could in principle be reconstructed from the kinematical edges of di-lepton mass distributions

(i.e. $\chi_2^0 \rightarrow \chi_1^0 \ell_i^\pm \ell_i^\mp$ can occur, and with a non-negligible number of events), we study slepton mass splittings, exploring the implications for LFV decays. From the comparison of the predictions for the two sets of observables (high- and low-energy) with the current experimental bounds and future sensitivities, one can either derive information about the otherwise unreachable seesaw parameters, or disfavour the type III SUSY seesaw as being the unique source of lepton flavour violation.

The paper is organised as follows: in section 2 we define the model, providing a brief overview on the implementation of a type III seesaw in the cMSSM. In section 3 we discuss the implications of this mechanism for low- and high-energy LFV observables. Our results are presented in section 4 where we study the different high- and low-energy observables in the seesaw case. This will also allow to draw some conclusions on the viability of a supersymmetric type III seesaw as the underlying mechanism of LFV. Further discussion is presented in the concluding section 5.

2 Type III SUSY seesaw

Under the hypothesis that neutrinos are Majorana particles, the smallness of their masses, as well as their mixings, can be explained via seesaw-like mechanisms due to the exchange of heavy states: fermionic singlets (type I), scalar triplets (type II) or fermionic triplets (type III). The three possible seesaw realisations can be easily embedded in the framework of supersymmetric models. However, if SUSY's appealing feature of gauge coupling (and gaugino mass) unification is to be preserved, the new particles present below the Grand Unified scale must belong to complete GUT representations. Under the assumption of an SU(5) gauge group, generating a neutrino mass matrix with at least two non-zero eigenvalues¹ requires the following multiplet content: two copies of **1** or **24** (type I and III, respectively) or $\overline{\mathbf{15}} + \mathbf{15}$ (type II). The addition of the non-singlet fields (i.e. the **15**- and the **24**-plets) has an important effect on the evolution of several fundamental parameters, especially on the β -functions for gauge and Yukawa couplings, as well as on the Renormalisation Group (RG) running of mass terms above the seesaw scale. At low-energies (electroweak scale) this translates into changes in the SUSY spectrum, leading to scenarios that can be significantly different from a minimal supergravity (mSUGRA) inspired (or minimal type I SUSY seesaw) scenario. In turn, this will have consequences concerning flavour observables and cosmological quantities like the dark matter relic density.

We consider in this study a generic framework where three families of triplet fermions, Σ_i , (as well as their superpartners) are added to the MSSM particle content [56]. Each one is embedded into a **24**-plet,² that decomposes under the SM gauge group, SU(3)×SU(2)×U(1), as

$$\begin{aligned} \mathbf{24} &= (8, 1, 0) + (3, 2, -5/6) + (3^*, 2, 5/6) + (1, 3, 0) + (1, 1, 0) \\ &= \widehat{G}_M + \widehat{X}_M + \widehat{\bar{X}}_M + \widehat{W}_M + \widehat{B}_M. \end{aligned} \quad (2.1)$$

¹Rank ≥ 2 neutrino mass matrices can also be obtained with a truly minimal heavy field content, via the inclusion of non-renormalisable operators in the superpotential (see, for example, [54, 55]).

²Among the representations of lower dimension, only the **24** does indeed contain a singlet hypercharge field.

The fermionic components of the last two terms in the above decomposition (\widehat{W}_M and \widehat{B}_M) have exactly the same quantum numbers of a fermionic triplet (Σ) and of a singlet right-handed neutrino (ν_R). It is then clear that if embedded into an SU(5) framework, the realisation of the type III seesaw will in general produce a mixture of type I and type III mechanisms.

In the unbroken SU(5) phase, the superpotential is given by

$$\mathcal{W}^{\text{SU}(5)} = \sqrt{2} \mathbf{\bar{5}}_{M_i} Y_{ij}^5 \mathbf{10}_{M_j} \mathbf{\bar{5}}_H - \frac{1}{4} \mathbf{10}_{M_i} Y_{ij}^{10} \mathbf{10}_{M_j} \mathbf{5}_H + \mathbf{5}_H \mathbf{24}_{M_i} Y_{ij}^N \mathbf{\bar{5}}_{M_j} + \frac{1}{4} \mathbf{24}_{M_i} M_{24ij} \mathbf{24}_{M_j}, \quad (2.2)$$

with i, j denoting generation (flavour) indices, and where we have not included the terms specifying the Higgs sector responsible for the breaking of SU(5). The Majorana mass term in eq. (2.2) is gauge invariant due to having the triplet superfields in the adjoint SU(2) representation. In the broken phase, in addition to the usual MSSM terms, the superpotential is given by:

$$\begin{aligned} \mathcal{W} = & \mathcal{W}^{\text{MSSM}} + \widehat{H}_2 \left(\widehat{W}_M Y_M - \sqrt{\frac{3}{10}} \widehat{B}_M Y_B \right) \widehat{L} + \widehat{H}_2 \widehat{X}_M Y_X \widehat{D}^c + \\ & + \frac{1}{2} \widehat{B}_M M_B \widehat{B}_M + \frac{1}{2} \widehat{G}_M M_G \widehat{G}_M + \frac{1}{2} \widehat{W}_M M_W \widehat{W}_M + \widehat{X}_M M_X \widehat{X}_M. \end{aligned} \quad (2.3)$$

After the heavy fields have been integrated out, and at lowest order in the expansion in $(v_2 Y_{B,W}/M_{B,W})^n$ (v_2 being the vacuum expectation value of H_2^0), one obtains the light neutrino mass matrix:

$$m_\nu \approx -v_2^2 \left(\frac{3}{10} Y_B^T M_B^{-1} Y_B + \frac{1}{2} Y_W^T M_W^{-1} Y_W \right), \quad (2.4)$$

where we have again omitted flavour indices. From the above formula, it is clear that we are indeed in the presence of a mixed type I and III seesaw, with contributions to m_ν arising from both the singlets ($\propto Y_B$) and SU(2) triplets ($\propto Y_W$). The model is further specified by $\mathcal{W}^{\text{MSSM}}$ and by the soft-SUSY breaking Lagrangian. Concerning the latter, we will furthermore assume a cMSSM framework, where mSUGRA-inspired universality conditions for the soft-breaking SUSY parameters are imposed at some very high-energy scale, which we take to be M_{GUT} . The MSSM part of the model is then defined by the usual 4 continuous parameters (the universal gaugino and scalar soft-breaking masses $M_{1/2}$ and m_0 , the universal trilinear coupling A_0 and the ratio of the Higgs vacuum expectation values, $\tan \beta = v_2/v_1$) and the sign of the bilinear μ -term in $\mathcal{W}^{\text{MSSM}}$, $\text{sign}(\mu)$.

One can further impose additional GUT scale SU(5)-motivated boundary conditions for the Yukawa couplings and Majorana masses appearing in eq. (2.3): $Y_B = Y_W = Y_X$ and $M_B = M_W = M_G = M_X$. Although the above parameters do run between the GUT scale and their corresponding decoupling scales, one has, to a very good approximation, that $Y_B \simeq Y_W$ and $M_B \simeq M_W$ as the heavy states decouple. At the seesaw scale (which we define to be $\approx M_B \simeq M_W$) m_ν is approximately given by

$$m_\nu \approx -v_2^2 \frac{4}{5} Y^{\nu T} M_N^{-1} Y^\nu, \quad (2.5)$$

where we have again used the simplifying notation $Y_B = Y_W = Y_N = Y^\nu$, $M_B = M_W = M_N$.

Up to an overall factor (4/5), one can still use the Casas-Ibarra parametrization [23] for the neutrino Yukawa couplings at the seesaw scale M_N ,

$$Y^\nu v_2 = i \sqrt{M_N^{\text{diag}}} R \sqrt{m_\nu^{\text{diag}}} U_{\text{MNS}}^\dagger. \quad (2.6)$$

In the above R is a complex orthogonal 3×3 matrix that encodes the possible mixings involving the heavy neutral states, in addition to those of the low-energy sector (i.e. U_{MNS}), and which is parametrized in terms of three complex angles θ_i ($i = 1, 2, 3$).

As extensively discussed in [56], the β -functions of the gauge couplings, as well as the running for soft gaugino and scalar masses, are strongly affected in type III seesaw models. In fact, RGE effects are behind the relatively small interval for M_N in a type III SUSY seesaw. Assuming that the triplet masses are degenerate ($M_{N_i} = M_{24}$), the interval is bounded from above, $M_{24} \lesssim 9 \times 10^{14}$ GeV, to comply with the atmospheric neutrino mass difference. On the other hand, for triplet masses below 10^{13} GeV, the running is such that one encounters Landau poles for the gauge couplings at the GUT scale, while tachyonic sfermions (especially the lighter stau and stop) can also arise for smaller values of the soft-SUSY breaking parameters.

As clear from the above discussion, the new distinctive features of a type III seesaw will likely be manifest in many phenomena. In what follows we discuss the new contributions of the type III SUSY seesaw for low-energy lepton flavour violation (e.g. to radiative decays such as $\mu \rightarrow e\gamma$), as well as for LFV at the LHC: in particular, we focus on the study of slepton mass splittings to probe deviations from the cMSSM and possibly derive information about the SUSY seesaw parameters.

3 Lepton flavour violation in a type III SUSY seesaw

As for the case of a type I SUSY seesaw, the non-trivial flavour structure of Y^ν at the GUT scale will induce (through the running from M_{GUT} down to the seesaw scale) flavour mixing in the otherwise approximately flavour conserving soft-SUSY breaking terms. In particular, there will be radiatively induced flavour mixing in the slepton mass matrices, manifest in the LL and LR blocks of the 6×6 slepton mass matrix; an analytical estimation using the leading order (LLog) approximation leads to the following corrections to the slepton mass terms [56]:

$$\begin{aligned} (\Delta m_L^2)_{ij} &= -\frac{9}{5} \frac{1}{8\pi^2} (3m_0^2 + A_0^2) (Y^{\nu\dagger} L Y^\nu)_{ij}, \\ (\Delta A_l)_{ij} &= -\frac{9}{5} \frac{3}{16\pi^2} A_0 Y_{ij}^l (Y^{\nu\dagger} L Y^\nu)_{ij}, \\ (\Delta m_E^2)_{ij} &\simeq 0; \quad L_{kl} \equiv \log \left(\frac{M_X}{M_{N_k}} \right) \delta_{kl}. \end{aligned} \quad (3.1)$$

When compared to the type I SUSY seesaw, the most important difference corresponds to a change in the overall factor (multiplying the $(Y^{\nu\dagger} L Y^\nu)_{ij}$ term). The above sources of flavour mixing will have an impact regarding lepton flavour non-universality and lepton

flavour violation in the charged slepton sector, potentially inducing sizable contributions to high- and low-energy LFV observables, as we proceed to discuss.

As mentioned in the Introduction, several LFV signals can be observable at the LHC, in strict relation with the $\chi_2^0 \rightarrow \chi_1^0 \ell^\pm \ell^\mp$ decay chains. As discussed in [45–50], in scenarios where the χ_2^0 is sufficiently heavy to decay via a real (on-shell) slepton, the process $\chi_2^0 \rightarrow \chi_1^0 \ell^\pm \ell^\mp$ is greatly enhanced while providing a very distinctive signal: same-flavour opposite-charged leptons with missing energy. The $\chi_2^0 \rightarrow \chi_1^0 \ell^\pm \ell^\mp$ decay chain thus offers a golden laboratory to study LFV at the LHC, via the following observables:

- (i) sizable widths for LFV decay processes like $\chi_2^0 \rightarrow \chi_1^0 \ell_i^\pm \ell_j^\mp$ [38, 41–44];
- (ii) multiple edges in di-lepton invariant mass distributions $\chi_2^0 \rightarrow \chi_1^0 \ell_i^\pm \ell_i^\mp$, arising from the exchange of a different flavour slepton \tilde{l}_j (in addition to the left- and right-handed sleptons, $\tilde{l}_{L,R}^i$);
- (iii) flavoured slepton mass splittings.

In order to optimise the reconstruction of the leptons’ momentum (which is expected to be easy, accounting for smearing effects in τ ’s [57, 58]) and, in addition, extract indirect information on the mass spectrum of the involved sparticles, the SUSY spectrum must comply with the requirements of a so-called “standard window”:

- (a) the spectrum is such that the decay chain $\chi_2^0 \rightarrow \tilde{\ell} \ell \rightarrow \chi_1^0 \ell \ell$, with intermediate real sleptons, is allowed;
- (b) it is possible to have sufficiently hard outgoing leptons: $m_{\chi_2^0} - m_{\tilde{\ell}_L, \tilde{\tau}_2} > 10 \text{ GeV}$.

In this case, the di-lepton invariant mass spectrum has a kinematical edge that might be measured with a very high precision (up to 0.1 %) [45–47]. Together with data arising from other observables, this information allows to reconstruct the slepton masses [45–50], and hence probe slepton mass universality or test LFV in the slepton sector. In particular, the relative slepton mass splittings, which are defined as

$$\frac{\Delta m_{\tilde{\ell}}(\tilde{\ell}_i, \tilde{\ell}_j)}{m_{\tilde{\ell}}} = \frac{|m_{\tilde{\ell}_i} - m_{\tilde{\ell}_j}|}{< m_{\tilde{\ell}_{i,j}} >}, \quad (3.2)$$

can be inferred from the kinematical edges with a sensitivity of $\mathcal{O}(0.1\%)$ [59] for $\tilde{e}_L - \tilde{\mu}_L$. It is important to stress that such sensitivities were obtained in dedicated studies conducted for a comparatively light SUSY spectrum - already excluded by the ATLAS [60] and the CMS collaborations [61]. In what follows, we will assume that, despite the heavier SUSY spectrum, a sensitivity of at least 1% can still be reached for the slepton mass splittings. Stau-smuon mass splittings ($\tilde{\mu}_L - \tilde{\tau}_2$) could also be used as an indicator of LFV.

Even in the absence of a seesaw mechanism, it is important to recall that universality between the third and first two slepton generations is broken due to LR mixing and to RGE effects proportional to the third generation lepton Yukawa coupling. However, in the

presence of flavour violation (as induced by the SUSY seesaw, see eqs. (3.1)), the mass differences between left-handed selectrons, smuons and staus can be potentially augmented.³ Similar to the case of a type I seesaw [51], the relative mass splittings between left-handed sleptons is approximately given by

$$\frac{\Delta m_{\tilde{\ell}}}{m_{\tilde{\ell}}}(\tilde{\ell}_i, \tilde{\ell}_j) \approx \frac{|(\Delta m_L^2)_{ij}|}{m_{\tilde{\ell}}^2} \quad (3.3)$$

where we have neglected LR mixing effects, as well as RGE contributions proportional to the charged lepton Yukawa coupling. In the $R = 1$ seesaw limit, where all flavour violation in Y^ν stems from the U_{MNS} (see eq. (2.6)), and assuming that the large flavour violating entries involving the second and third generation constitute the dominant source of mixing⁴ (and are thus at the origin of the slepton mass differences), one can further relate the $\tilde{e}_L - \tilde{\mu}_L$ and the $\tilde{\mu}_L - \tilde{\tau}_2$ mass differences [51]:

$$\frac{\Delta m_{\tilde{\ell}}}{m_{\tilde{\ell}}}(\tilde{e}_L, \tilde{\mu}_L) \approx \frac{1}{2} \frac{\Delta m_{\tilde{\ell}}}{m_{\tilde{\ell}}}(\tilde{\mu}_L, \tilde{\tau}_2). \quad (3.4)$$

As discussed in [51], in the framework of a type I seesaw, the slepton mass differences can be sufficiently large as to be within the reach of LHC sensitivity.

Before proceeding, let us briefly notice that, depending on the amount of flavour violation, one can be led to regimes where two non-degenerate mass eigenstates have almost identical flavour content (maximal flavour mixing). To correctly interpret a mass splitting between sleptons with quasi-degenerate flavour content, one has to introduce an “effective” mass

$$m_i^{(\text{eff})} \equiv \sum_{X=\tilde{\tau}_2, \tilde{\mu}_L, \tilde{e}_L} m_{\tilde{X}} \left(|R_{Xi_L}^{\tilde{L}}|^2 + |R_{Xi_R}^{\tilde{L}}|^2 \right), \quad (3.5)$$

where $R^{\tilde{L}}$ is the matrix that diagonalizes the 6×6 slepton mass matrix. The effective mass splittings are then defined as

$$\left(\frac{\Delta m}{m} \right)^{(\text{eff})}(\tilde{\ell}_i, \tilde{\ell}_j) \equiv \frac{2 |m_i^{(\text{eff})} - m_j^{(\text{eff})}|}{m_i^{(\text{eff})} + m_j^{(\text{eff})}}. \quad (3.6)$$

The seesaw-generated flavour violating entries of eqs. (3.1) will also give rise to low-energy LFV phenomena, such as radiative $\ell_i \rightarrow \ell_j \gamma$ decays, which are induced by 1-loop diagrams via the exchange of gauginos and sleptons. These can be described by the effective Lagrangian [18],

$$\mathcal{L}_{\text{eff}} = e \frac{m_{\ell_i}}{2} \bar{\ell}_i \sigma_{\mu\nu} F^{\mu\nu} (A_L^{ij} P_L + A_R^{ij} P_R) \ell_j + \text{H.c.}, \quad (3.7)$$

³Slepton mass splittings as a probe of LFV have also been studied in the context of scenarios with an effective parametrization of flavour violation [62].

⁴Assuming $|(\Delta m_L^2)_{23}| \gg |(\Delta m_L^2)_{21,31}|$ in the limit $R = 1$ is a very good approximation, both in the case of degenerate and of hierarchical seesaw mediator spectra.

where $P_{L,R} = \frac{1}{2}(1 \mp \gamma_5)$ are the usual chirality projectors and the couplings A_L and A_R arise from loops involving left- and right-handed sleptons, respectively. Using eq. (3.7), the branching ratio $\ell_i \rightarrow \ell_j \gamma$ is given by

$$\text{BR}(\ell_i \rightarrow \ell_j \gamma) = \frac{48\pi^3 \alpha}{G_F^2} \left(|A_L^{ij}|^2 + |A_R^{ij}|^2 \right) \text{BR}(\ell_i \rightarrow \ell_j \nu_i \bar{\nu}_j). \quad (3.8)$$

where G_F is the Fermi constant and α is the electromagnetic coupling constant. In our numerical calculation we use the exact expressions for A_L and A_R .⁵ However, for an easier understanding of the numerical results, we note that the relations between these couplings and the slepton soft-breaking masses are approximately given by

$$\begin{aligned} |A_L^{ij}| &\sim \frac{|(\Delta m_L^2)_{ij}| \tan \beta}{m_{\text{SUSY}}^4} \simeq \left| \frac{9}{5} \frac{\tan \beta}{8 \pi^2} \frac{(3 m_0^2 + A_0^2)}{m_{\text{SUSY}}^4} (Y^{\nu\dagger} L Y^\nu)_{ij} \right|, \\ A_R^{ij} &\sim \frac{(\Delta m_E^2)_{ij} \tan \beta}{m_{\text{SUSY}}^4} \simeq 0, \end{aligned} \quad (3.9)$$

where m_{SUSY} denotes a generic (average) SUSY mass and where we have used eqs. (3.1).

A clear understanding of the correlation of high- and low-energy observables in the framework of the SUSY seesaw can be obtained when one directly compares cLFV observables dominated by the same flavour violating entry in the slepton mass matrix. As an example, we illustrate below the correlation between the $\text{BR}(\tau \rightarrow \mu \gamma)$ and the $\tilde{\mu}_L - \tilde{\tau}_2$ mass splittings, proportional to the $\tilde{e}_L - \tilde{\mu}_L$ mass difference, which is the one relevant to our study. Working in the case of hierarchical triplets, and in the limit $\theta_{13} \approx 0$, one has

$$\frac{\text{BR}(\tau \rightarrow \mu \gamma)}{\text{BR}(\tau \rightarrow \mu \nu_\tau \bar{\nu}_\mu)} \propto L_{33} M_{N_3} m_{\nu_3} \sin 2\theta_{23} \times \frac{\Delta m_{\tilde{\ell}}}{m_{\tilde{\ell}}}(\tilde{\mu}_L, \tilde{\tau}_2), \quad (3.10)$$

where we have omitted a dimensionful prefactor (function of electroweak and mSUGRA parameters). Equally interesting LFV observables are $\mu - e$ conversions in heavy nuclei, as they offer challenging experimental prospects: the possibility of improving experimental sensitivities to values as low as $\sim 10^{-18}$ renders this observable an extremely powerful probe of LFV in the muon-electron sector. In the limit of photon-penguin dominance, the conversion rate $\text{CR}(\mu - e, N)$ and $\text{BR}(\mu \rightarrow e \gamma)$ are strongly correlated, since both observables are sensitive to the same leptonic mixing parameters [39].

The type III SUSY seesaw leads to scenarios of LFV that are considerably more constrained than what occurs for the type I SUSY seesaw and moreover, a type III SUSY seesaw in general implies larger contributions to LFV observables [56]. A direct comparison between type I and type III seesaws is hampered by the fact that identical mSUGRA boundary conditions lead to distinct low-energy SUSY spectra for each different seesaw realisation (the running of the soft-breaking parameters in the type III seesaw typically leads to a lighter spectrum [56], and cannot be decorrelated from the amount of radiatively induced LFV). However, one can nevertheless stress that in the type I, one can still choose

⁵The exact formulae for the branching ratios of the radiative LFV decays, as used in our numerical computation, can be found, for example, in [63].

distinct regimes that allow to suppress LFV (e.g. by lowering the seesaw scale), while the tightly constrained type III case does not allow such possibilities.

Before proceeding to the numerical analysis, a brief comment regarding potential flavour violating effects in the quark sector is in order: as seen from eq. (2.3), the right-handed quark superfields couple to \hat{H}_2 and to the heavy fields, \widehat{X}_M , via Y_X . These non-diagonal couplings will induce, through RGE running, flavour non-diagonal entries in the down-squark mass matrix, similar to what occurs in the slepton mass matrices, see eq. (3.1). In principle, this can induce large contributions to hadronic flavour changing neutral currents, due to the FV exchange of squarks and gluinos. Although a numerical discussion of these effects clearly lies beyond the scope of this (lepton-dedicated) analysis, we expect no conflict with experimental bounds, since (as will be numerically confirmed in the following section) squarks and gluinos are quite heavy in the present model.

4 Numerical results and discussion

For the numerical computation, we have used the public code SPHENO (v3.beta.51) [64] to carry out the numerical integration of the RGEs. The RGEs of the SU(5) type III SUSY seesaw were calculated at 2-loop level in [56], using the public code SARAH [65]. SPHENO further computes the sparticle and Higgs spectrum, as well as the various low-energy LFV observables. The dark matter relic density is evaluated through a link to MICROMEGAS v2.2 [66].

Regarding low-energy neutrino data, current (best-fit) analyses favour the following intervals for the mixing angles [67]

$$\theta_{12} = (34.4 \pm 1.0)^\circ, \quad \theta_{23} = (42.8^{+4.7}_{-2.9})^\circ, \quad \theta_{13} = (5.6^{+3.0}_{-2.7})^\circ (\leq 12.5^\circ), \quad (4.1)$$

while for the mass-squared differences one has

$$\Delta m_{21}^2 = (7.6 \pm 0.2) \times 10^{-5} \text{ eV}^2, \quad \Delta m_{31}^2 = \begin{cases} (-2.36 \pm 0.11) \times 10^{-3} \text{ eV}^2 \\ (+2.46 \pm 0.12) \times 10^{-3} \text{ eV}^2 \end{cases}, \quad (4.2)$$

where the two ranges for Δm_{31}^2 correspond to inverted and normal neutrino spectra. In our analysis, and unless otherwise stated, we will assume a hierarchical spectrum for the light neutrinos, and take the lightest neutrino mass to be $m_{\nu_1} = 10^{-4} \text{ eV}$. In table 1 we summarise the current bounds and the future sensitivities of dedicated experimental facilities, for the low-energy LFV observables considered in our numerical discussion.

In the first part of the analysis we assume a degenerate spectrum for the three families of triplet fermions. Moreover, we consider the conservative limit⁶ in which flavour violation solely arises from the U_{MNS} leptonic mixing matrix, i.e. $R = 1$ in eq. (2.6). Leading to the results displayed in this section, we have taken into account all available LEP and Tevatron

⁶In general, the limit $R = 1$ translates into a “conservative” limit for flavour violation: apart from possible cancellations, and for a fixed seesaw scale, this limit typically provides a lower bound for the amount of generated LFV.

LFV process	Present bound	Future sensitivity
$\text{BR}(\mu \rightarrow e\gamma)$	1.2×10^{-11} [68]	10^{-13} [69]
$\text{BR}(\tau \rightarrow \mu\gamma)$	4.5×10^{-8} [70]	10^{-9} [71]
$\text{CR}(\mu - e, \text{Ti})$	4.3×10^{-12} [68]	$\mathcal{O}(10^{-16})$ ($\mathcal{O}(10^{-18})$) [72] ([73])

Table 1. Present bounds and future sensitivities for several LFV observables.

bounds on the Higgs boson and SUSY spectrum [68, 74–76], as well as the most recent results on negative SUSY searches from the LHC collaborations [60, 61].

Concerning the WMAP7 bound for the observed dark matter relic density [17],

$$0.0941 \lesssim \Omega h^2 \lesssim 0.1277, \quad (4.3)$$

we do not systematically impose it as a viability requirement in our analysis. Nevertheless, we do require the lightest neutralino to be the lightest SUSY particle (LSP). We will return to this issue at a later stage.

Let us then begin our discussion by investigating how the requirements of a “standard window”, as well as compatibility with experimental bounds, constrain the type III SUSY seesaw parameter space in the case of degenerate fermion triplets (i.e., $M_{N_i} = M_{24}$).

On the left-hand side of figure 1, we display the $m_0 - M_{1/2}$ parameter space for a type III SUSY seesaw, taking $A_0 = 0$, $\tan\beta = 10$, and a seesaw scale $M_{24} \sim 5 \times 10^{14}$ GeV, setting also $\theta_{13} = 0.1^\circ$. The excluded (shaded) areas correspond to a charged LSP, to the violation of collider constraints on the Higgs and sparticle spectrum, and to kinematically disfavoured regimes (kinematically closed $\chi_2^0 \rightarrow \tilde{\ell}\ell$ channel, excessively soft outgoing leptons, etc.). The requirements of a “standard window” (see section 3) are fulfilled on the central white region. For this choice of SUSY seesaw parameters, a large part of the latter viable region is excluded since it is associated with an excessively large $\mu \rightarrow e\gamma$ branching ratio, as can be verified from the isocurves for the $\text{BR}(\mu \rightarrow e\gamma)$. Additional isocurves (dashed-dotted lines) denote $\text{BR}(\chi_2^0 \rightarrow \chi_1^0 \mu\mu)$. In the region complying with the “standard window” requirements, the latter range from 5% to 7%, so that even under optimal conditions (i.e. $\sqrt{s} = 14$ TeV and an integrated luminosity of 100 fb^{-1}), one could only expect some 10 to 1000 events. As an interesting example, we point out that in the dark matter compatible region of figure 1, one can expect over $\mathcal{O}(1500)$ events. If squarks are not too heavy to be produced, then LFV from χ_2^0 decay chains (with the neutralino produced from squark decay) might still be studied in the higher luminosity and higher energy phase of the LHC. In what follows we will be assuming that the observed number of events will indeed allow to reconstruct the end-points of the di-lepton distributions.

Concerning dark matter, it is important to notice that, although the requirements imposed on the $\chi_2^0 \rightarrow \tilde{\ell}\ell$ decay usually lead to a region where the correct dark matter relic density could in principle be obtained from co-annihilations of the LSP with the next-to-LSP (NLSP), finding points for which Ωh^2 is indeed in agreement with WMAP7 data proves to be challenging. For the particular SUSY seesaw configuration investigated in figure 1, we verify that the regions where one finds the correct dark matter relic density

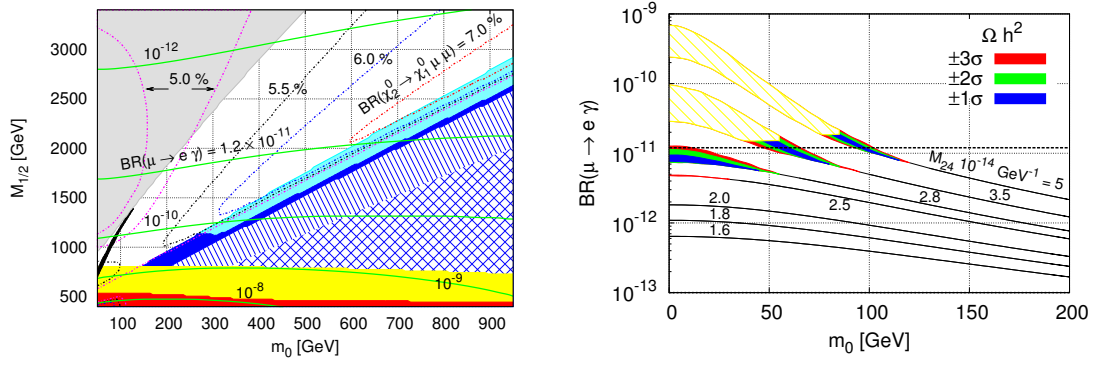


Figure 1. On the left, $m_0 - M_{1/2}$ plane (in GeV), with $A_0 = 0$, $\tan\beta = 10$, for a seesaw scale $M_{24} \sim 5 \times 10^{14}$ GeV and $\theta_{13} = 0.1^\circ$. The shaded region on the left is excluded due to the presence of a charged LSP, while the yellow (red) region is excluded in view of $m_{h_1^0}$ bounds ($m_{h_1^0}$ and LHC bounds). Several regions do not fulfil the “standard window” requirements: solid regions correspond to having $m_{\chi_2^0} < m_{\tilde{\ell}_L} + 10$ GeV (cyan) and $m_{\chi_2^0} < m_{\tilde{\tau}_2} + 10$ GeV (blue). The dashed blue region corresponds to $m_{\chi_2^0} < m_{\tilde{\ell}_L, \tilde{\tau}_2}$ while blue crosses correspond to $m_{\chi_2^0} < m_{\tilde{\tau}_1} + m_\tau$. The centre white region denotes the parameter space obeying the “standard window” constraint. Green lines denote isocurves for $\text{BR}(\mu \rightarrow e\gamma)$, while the dashed-dotted lines correspond to different values of $\text{BR}(\chi_2^0 \rightarrow \chi_1^0 \mu\mu)$ as indicated in the plot. A small black region in the lower left corner corresponds to a WMAP7 compatible χ_1^0 relic density. On the right panel, $\text{BR}(\mu \rightarrow e\gamma)$ as a function of m_0 (in GeV), for $A_0 = 0$, $\tan\beta = 5$, $\theta_{13} = 0.1^\circ$ and several values of M_{24} : 1.6×10^{14} GeV $\lesssim M_{24} \lesssim 5 \times 10^{14}$ GeV (from lower to upper curves). Horizontal lines correspond to the current bound and future sensitivity. The yellow gridded region is excluded due to violation of $m_{h_1^0}$ bounds. The colour code denotes compatibility with the WMAP7 bounds on Ωh^2 .

are already excluded due to having an excessively large $\text{BR}(\mu \rightarrow e\gamma)$. Although viable DM scenarios in the type III SUSY seesaw are indeed very constrained [56], regions can be found where either by a different choice of seesaw parameters (e.g. setting δ , the Dirac phase in U_{MNS} , $\delta = \pi$) or for smaller $\tan\beta$ values, a viable Ωh^2 can be obtained, but still in association with a considerable fine tuning of the parameters. This is illustrated on the right-hand side plot of figure 1 for $\tan\beta = 5$, where we display $\text{BR}(\mu \rightarrow e\gamma)$ as a function of m_0 for several (7) choices of the seesaw scale, 1.6×10^{14} GeV $\lesssim M_{24} \lesssim 5 \times 10^{14}$ GeV. When compatibility with the WMAP7 3σ interval for Ωh^2 is indeed possible, $M_{1/2}$ has been varied (corresponding to the coloured solid regions as well as the gridded ones - which are already excluded by collider constraints); else, we display the value of $M_{1/2}$ that minimises the deviation from the WMAP7 3σ interval (black curves). Typically, the correct relic density is obtained for nearly degenerate LSP and NLSP.

Contrary to the type I seesaw, where the requirements of observing the $\chi_2^0 \rightarrow \chi_1^0 \ell\ell$ chain did not significantly alter the expected low-energy SUSY spectrum, important changes are expected in the type III seesaw, especially due to the (strong) running of the gaugino masses. Moreover, and as discussed previously, the allowed interval for the triplet masses (M_{24}) is also severely constrained. To illustrate the impact of a “standard window” on the spectrum, we display in figure 2 the (geometrically) averaged squark masses

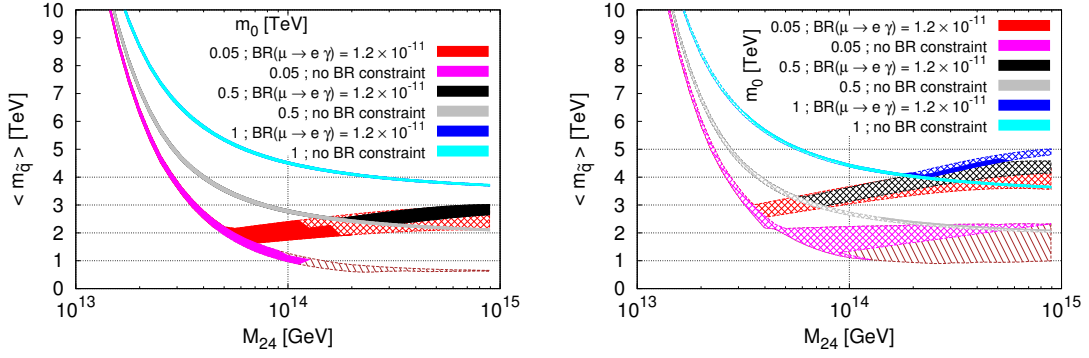


Figure 2. Average squark mass range (in TeV) as a function of the triplet mass (in GeV), for different values of m_0 : 50 GeV (blue/cyan), 500 GeV (black/grey) and 1 TeV (red/pink), the colour code further denoting imposing/not imposing the bound on $\text{BR}(\mu \rightarrow e\gamma)$. Gridded regions correspond to cases where one has a charged LSP. The brown region is excluded due to violation of LHC or $m_{h_1^0}$ bounds. The left (right) figure corresponds to $\tan\beta = 10$ (40). In both cases, $\theta_{13} = 0.1^\circ$, $A_0 = \{-1, 0, 1\}$ TeV, with $M_{1/2}$ set to the lowest possible value complying with the requirement of a “standard window”.

as a function of the triplet mass, for different values of m_0 . We consider two regimes of $\tan\beta$, $\tan\beta = 10, 40$. For each point a scan over $M_{1/2}$ is conducted to determine its lowest possible value complying with the requirement of a “standard window”. We also differentiate between the ranges allowed with and without applying the current bound on $\text{BR}(\mu \rightarrow e\gamma)$. Regarding mixings in the neutrino sector, we again work in the limit $R = 1$ and set $\theta_{13} = 0.1^\circ$.

As can be seen from figure 2, and as hinted on section 2, the allowed interval for the seesaw scale (here represented by M_{24}) ranges from 10^{13} GeV to just below 10^{15} GeV, corresponding to the results of [56]. It is worth emphasising that there are regions where, in addition to complying with all accelerator and neutrino data, the type III seesaw still leads to scenarios of LFV in agreement with low-energy data (the most stringent constraint arising from the $\mu \rightarrow e\gamma$ decay). This diverges from the findings of [56], where only very light SUSY spectra were considered. Regimes of heavier sparticles (large $M_{1/2}$ and m_0) are clearly preferred, further suggesting that if within LHC reach, the latter spectra would only be observable for $\sqrt{s} = 14$ TeV. It is important to remark that, even for a regime of small m_0 , we are always led to a very heavy SUSY spectrum (here represented by a geometrical average of the squark masses). Complying with all the above requirements implies that even for m_0 as low as 50 GeV, one must have $\langle m_{\tilde{q}} \rangle^{\min} \sim 2$ TeV (and around 1.5 TeV for the limiting case of $m_0 = 0$). By itself, this result is important in the sense that should any light SUSY spectrum be discovered at the LHC in association with the $\chi_2^0 \rightarrow \tilde{\ell}\ell$ decay chain, this would strongly suggest that a type III seesaw is not at work. It is also important to notice that the steep increase of $\langle m_{\tilde{q}} \rangle$ for lower values of M_{24} is a direct consequence of having imposed the requirement of a “standard window”. In particular the strong running of M_2 would imply that for lower M_{24} the mass of the sleptons would be much larger than that of the neutralinos, thus preventing the cascade decay $\chi_2^0 \rightarrow \tilde{\ell}\ell$.

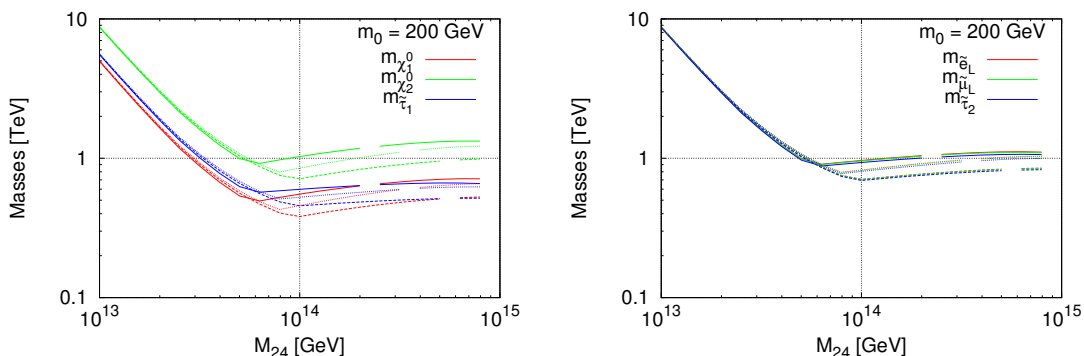


Figure 3. Gaugino and slepton masses (in TeV) as a function of the triplet mass, M_{24} (in GeV), for $m_0 = 200$ GeV. On the left, $m_{\chi_{1,2}^0}$ and $m_{\tilde{\tau}_1}$; on the right $m_{\tilde{e}_L}$, $m_{\tilde{\mu}_L}$ and $m_{\tilde{\tau}_2}$. We have taken $\tan\beta = 10$ and set $\theta_{13} = 0.1^\circ$. $M_{1/2}$ is set to the lowest possible value complying with the requirement of a “standard window” and with the bound on $\text{BR}(\mu \rightarrow e\gamma)$. In both cases, the different lines correspond to distinct values of A_0 : -1 TeV (full), 0 (dashed), and 1 TeV (dotted). An interrupted line signals the onset of a charged LSP region.

Increasing the value of $\tan\beta$ has an effect on the SUSY contributions to the LFV observables (which grow with $\tan^2\beta$, see eq. (3.9)), implying that larger values of the SUSY spectrum (and hence of $M_{1/2}$) are required in order to comply with the experimental constraints. Furthermore, the augmentation of the LR mixing in the stau sector implies that having a neutral LSP becomes increasingly difficult. For $\tan\beta = 40$, as depicted on the right-hand side of figure 2, the allowed regions are extremely reduced: only a thin blue band (corresponding to $m_0 = 1$ TeV) survives all constraints. To further clarify and illustrate the above discussion regarding the dependence of the sparticle spectrum on the seesaw scale (under the requirements of a “standard window” and compatibility with experimental bounds), we present on figure 3 the electroweak gaugino and slepton masses as a function of the triplet mass (M_{24}), also explicitly denoting the value of A_0 in each case. Being essentially driven by $M_{1/2}$, the running of their values is similar to that of the (averaged) squark masses.

Finally, let us notice that variations of the still unknown Chooz angle, θ_{13} , have a comparatively small impact: they only contribute to some of the LFV observables and compatibility with the experimental bound is easily recovered through a minor augmentation of $M_{1/2}$, which in turn leads to a heavier sparticle spectrum (for fixed values of m_0).

We now focus our discussion on the slepton mass differences, as potentially measurable at the LHC. We recall that, although the SUSY spectra are typically very heavy, we will assume that the expected (conservative) sensitivities for the slepton mass splittings are of $\mathcal{O}(0.1\%)$ for $\Delta m_{\tilde{\ell}}/m_{\tilde{\ell}}$ ($\tilde{e}, \tilde{\mu}$), as proposed in [59]. In figures 4 we display the effective slepton mass splittings $\tilde{e}_L - \tilde{\mu}_L$ as a function of the seesaw scale, for the same parameter scan as in figures 2. For completeness, we also display the same information concerning the $\tilde{\mu}_L - \tilde{\tau}_2$ mass difference. One verifies that $\Delta m_{\tilde{\ell}}/m_{\tilde{\ell}}$ ($\tilde{e}_L, \tilde{\mu}_L$) can be as large as 3% ($\Delta m_{\tilde{\ell}}/m_{\tilde{\ell}}$ ($\tilde{\mu}_L, \tilde{\tau}_2$) $\sim 5\%$), for the maximal values of the seesaw scale, and for large m_0 regimes (where the largest amount of flavour violation, still compatible with experimental

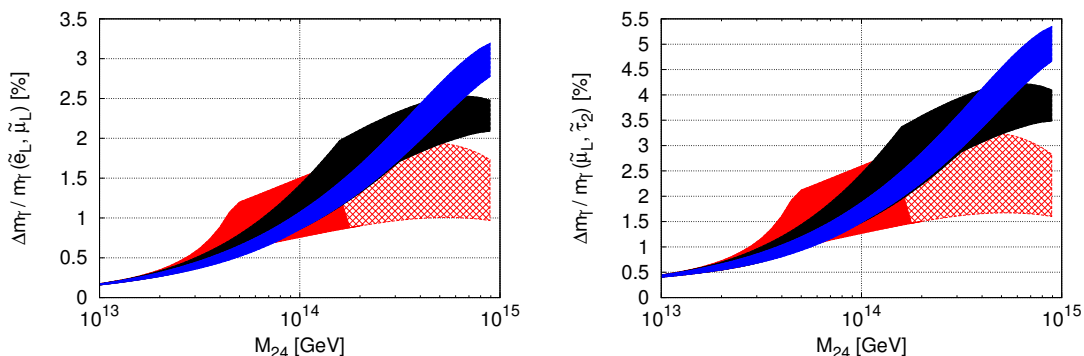


Figure 4. On the left, $\tilde{e}_L - \tilde{\mu}_L$ mass difference (normalised to an average slepton mass) as a function of the triplet mass, M_{24} (in GeV). On the right, $\tilde{\mu}_L - \tilde{\tau}_2$ effective mass difference (normalised to the corresponding average slepton mass) also as a function of the seesaw scale. In both cases we take $\tan\beta = 10$, $\theta_{13} = 0.1^\circ$, and consider different values of m_0 : 50 GeV (red), 500 GeV (black), and 1 TeV (blue). Gridded regions correspond to a charged LSP. For each point one varies $A_0 = \{-1, 0, 1\}$ TeV, while $M_{1/2}$ is set to the lowest possible value complying with the requirement of a “standard window” and with the bound on $\text{BR}(\mu \rightarrow e\gamma)$.

bounds and with the requirements of a “standard window”, occurs). The effect of larger values of $\tan\beta$ would only be visible in slightly larger $\tilde{\mu}_L - \tilde{\tau}_2$ mass splittings (mostly in association with larger LR mixings in the stau sector), $\Delta m_{\tilde{\ell}}/m_{\tilde{\ell}}(\tilde{\mu}_L, \tilde{\tau}_2) \lesssim 7\%$. In all cases, the viable regions in the parameter space would be much smaller, as mentioned before.

When compared to a type I SUSY seesaw (see [51]), one realises that the maximal values of the slepton mass splittings are slightly smaller, which is a consequence of the somewhat heavier SUSY spectrum. Concerning the mass splittings of right-handed sleptons, and analogous to the type I case, one finds a very small effect: in fact, for the parameter space surveyed in figure 4 (and always under the imposition of a “standard window” as well as compatibility with collider constraints), $\Delta m_{\tilde{\ell}}/m_{\tilde{\ell}}(\tilde{\mu}_R, \tilde{e}_R) \lesssim 0.1\%$.

Finally, assuming that selectron-smuon slepton mass differences are measured close to their maximal values, i.e. $\sim 3\%$ for $\tilde{\mu}_L - \tilde{e}_L$, so that they are within reach of LHC measurement, and that the reconstructed value of m_0 is found to be large (around 1 TeV) then, as seen from figures 4, this would suggest that the seesaw scale would be $M_{24} \sim 10^{15}$ GeV (for the limiting case $R = 1$). A similar seesaw scale could be inferred from a possible measurement of $\Delta m_{\tilde{\ell}}/m_{\tilde{\ell}}(\tilde{\mu}_L, \tilde{\tau}_2) \sim 5\%$ (i.e. close to its maximal value).

In figure 5 we present the comparison of the $\tilde{e}_L - \tilde{\mu}_L$ and $\tilde{\mu}_L - \tilde{\tau}_2$ mass differences, as well as their ratio, as a function of the seesaw scale. This is particularly useful to confirm that, as suggested by the analytical discussion of section 3, and similar to what occurs for a type I SUSY seesaw, the mass differences are strongly correlated. Moreover, this does indeed confirm that, as previously hinted, $\Delta m_{\tilde{\ell}}(\tilde{e}_L, \tilde{\mu}_L)$ is driven by the $(\Delta m_{\tilde{L}}^2)_{23}$ entry in the slepton mass matrix. With the exception of the regions corresponding to smaller values of M_{24} , the relation $\Delta m_{\tilde{\ell}}/m_{\tilde{\ell}}(\tilde{e}_L, \tilde{\mu}_L) \approx \mathcal{O}(1/2) \Delta m_{\tilde{\ell}}/m_{\tilde{\ell}}(\tilde{\mu}_L, \tilde{\tau}_2)$ (eq. (3.4)) typically holds to a very good approximation (with corrections due to fact that flavour conserving radiative corrections driven by the tau Yukawa coupling now play a non-negligible rôle). For lower

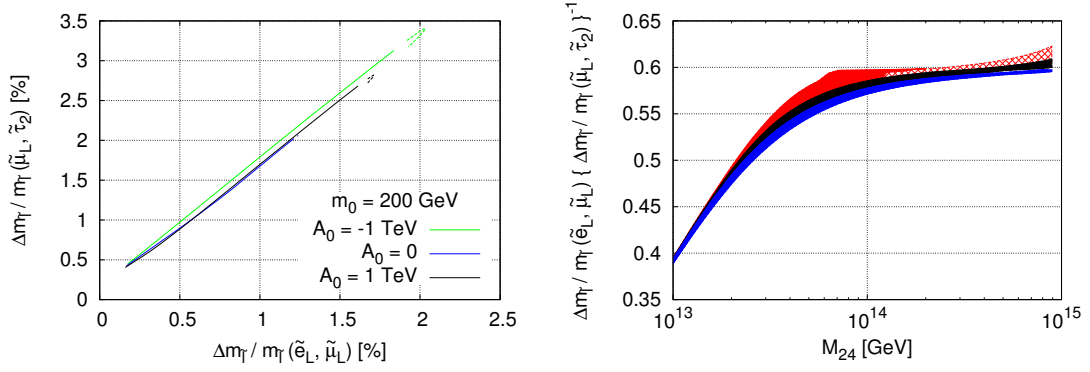


Figure 5. On the left, $\Delta m_{\tilde{\ell}}/m_{\tilde{\ell}}(\tilde{\mu}_L, \tilde{\tau}_2)$ as a function of $\Delta m_{\tilde{\ell}}/m_{\tilde{\ell}}(\tilde{e}_L, \tilde{\mu}_L)$, for $m_0 = 200$ GeV, $\tan \beta = 10$, $\theta_{13} = 0.1^\circ$ and taking $A_0 = \{-1, 0, 1\}$ TeV (green, blue and black lines, respectively). An interrupted (dashed) line signals the onset of a charged LSP regime towards larger values of the mass splittings. On the right, ratio of slepton mass differences, $\Delta m_{\tilde{\ell}}(\tilde{e}_L, \tilde{\mu}_L)/\Delta m_{\tilde{\ell}}(\tilde{\mu}_L, \tilde{\tau}_2)$ (normalised to the corresponding average slepton mass), as a function of the triplet mass (in GeV), for different values of m_0 , with $\tan \beta = 10$, $A_0 = \{-1, 0, 1\}$ TeV and $\theta_{13} = 0.1^\circ$. Scan and colour code as in figure 4.

values of the seesaw scale, where the requirement of a “standard window” (i.e. $\chi_2^0 \rightarrow \tilde{\ell}\ell$ decay, with hard outgoing leptons) forces a rapid increase of $M_{1/2}$, a small deviation to this strict correlation is observed. This can also be seen in the left-hand side of figure 5, zooming into the lower end of the lines. We have verified that this behaviour occurs irrespective of the value of θ_{13} and for all $\tan \beta$ regimes (provided that the regions are phenomenologically and experimentally viable).

The correlation of low- and high-energy LFV observables is explored in figure 6, where we present $\text{BR}(\mu \rightarrow e\gamma)$ and $\text{BR}(\tau \rightarrow \mu\gamma)$ as a function of the $\tilde{e}_L - \tilde{\mu}_L$ slepton mass difference, taking $m_0 = 100$ GeV, and considering different values of the triplet scale, M_{24} . We also provide additional information about the $\text{CR}(\mu - e, \text{Ti})$. As seen from both panels of figure 6, only a small region of the scanned parameter space complies with the requirements of a “standard window” while being in agreement with the several experimental and phenomenological constraints. Similar to what occurs for a type I SUSY seesaw, larger, negative values of A_0 translate into larger mass splittings. The maximal amount of flavour violation, both regarding radiative decays and slepton mass splittings, is obtained for: (i) a seesaw scale as large as possible (without violating perturbativity arguments, specifically on Y^ν), as can be understood from eqs. (2.6), (3.1); (ii) lower values of $M_{1/2}$ (leading to a lighter SUSY spectrum, see eq. (3.9)). Regarding the $\tau \rightarrow \mu\gamma$ decays, as can be seen from the right panel of figure 6, the regions in parameter space associated with $\text{BR}(\tau \rightarrow \mu\gamma)$ within the sensitivity of SuperB are in fact excluded by the present bounds on $\mu \rightarrow e\gamma$ decays. Although we do not present the corresponding results, a similar study with $m_0 = 1$ TeV leads to scenarios of somewhat larger mass splittings, and smaller branching ratios for the radiative decays (due to the much heavier spectrum). It is nevertheless interesting to remark that in this regime of very large m_0 , one can have maximal mixings in the lightest slepton - now a composition of $\tilde{\tau}_L$, $\tilde{\tau}_R$ and $\tilde{\mu}_L$ - possibly leading to scenarios of very large mass splittings (albeit for a tiny fraction of the parameter space).

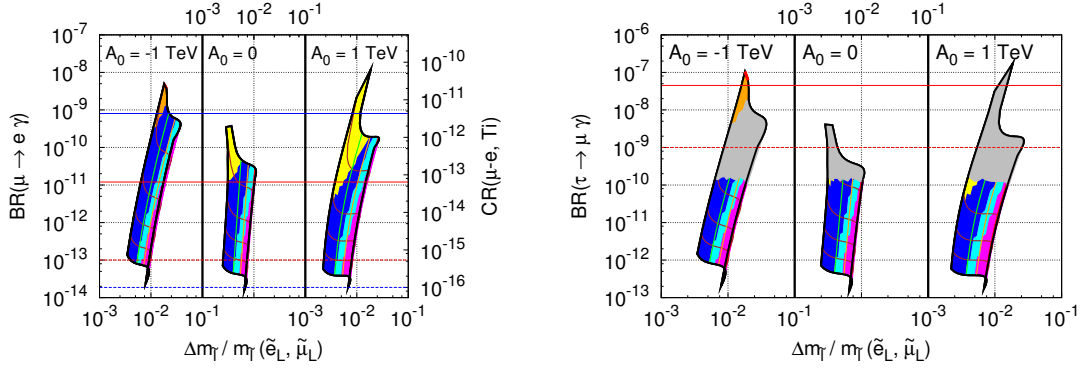


Figure 6. $\text{BR}(\mu \rightarrow e\gamma)$ and $\text{BR}(\tau \rightarrow \mu\gamma)$ as a function of the $\tilde{e}_L - \tilde{\mu}_L$ slepton mass difference (normalised to an average slepton mass), corresponding to the left- and right-hand side panels. In both cases we have set $m_0 = 100 \text{ GeV}$, $\tan\beta = 10$ and $\theta_{13} = 0.1^\circ$, and considered different values of the triplet scale M_{24} and of $M_{1/2}$. Each sub-panel corresponds to a distinct choice of A_0 . Cyan regions correspond to fulfilling the requirements of a “standard window”. The bounds on $m_{h_1^0}$ are violated in the yellow regions, LHC bounds on SUSY spectrum are violated in orange regions, while red regions are excluded due to both. Further excluded regions are due to failing to meet the kinematical constraints (blue), having a charged LSP (magenta) or violating another LFV bound (grey). Inset into each plot are “horizontal” isolines for $M_{1/2}$ (ranging from 1.5 TeV to 6 TeV, from top to bottom) and “vertical” isolines for M_{24} : from left to right, 10^{13} GeV to $9 \times 10^{14} \text{ GeV}$. The secondary y-axis on the left-hand panel illustrates the corresponding values of $\text{CR}(\mu - e, \text{Ti})$. Horizontal lines denote the current experimental bounds (full) and future sensitivities (dashed).

Assuming that a type III seesaw is indeed the only source of LFV, and given the extremely constrained parameter space, one finds that in the conservative case of $R = 1$, the corresponding slepton mass splittings will always lie around the % level, and thus appear to be potentially measurable at the LHC. Furthermore, these mass splittings correspond to values of $\text{BR}(\mu \rightarrow e\gamma)$ well within the expected sensitivity of MEG (or even already ruled out by current searches). In fact, the expected large values of $\text{BR}(\mu \rightarrow e\gamma)$ suggest that if indeed such a scenario is at work, MEG should see a signal in the very near future. The regions lying below MEG sensitivity still have an associated $\text{CR}(\mu - e, \text{Ti})$ within the reach of PRISM/PRIME, but they correspond to considerably smaller regions in parameter space.

We now consider more general scenarios of non-degenerate spectrum for the heavy triplets. In order to investigate this regime, we fix the heaviest (lightest) triplet mass to the upper (lower) limits of the M_{24} interval previously obtained, and allow the next-to-lightest triplet mass to vary between the latter limits. For such a non-degenerate triplet spectrum, we display in figure 7 an analogous study to that of figure 6 (same choice of the SUSY parameters, still working in the limiting case of $R = 1$). As can be observed, the area complying with all requirements (cyan band) is now comparatively larger. The $\tilde{e}_L - \tilde{\mu}_L$ slepton mass differences are also enhanced when compared to the degenerate case: for all three regimes of $A_0 = -1, 0, 1 \text{ TeV}$, one has $1\% \lesssim \Delta m_{\tilde{\ell}}/m_{\tilde{\ell}} (\tilde{e}_L, \tilde{\mu}_L) \lesssim 10\%$. Remarkably, one can have $\Delta m_{\tilde{\ell}}/m_{\tilde{\ell}} (\tilde{e}_L, \tilde{\mu}_L) \sim 5\%$, in agreement with current bounds on $\text{BR}(\mu \rightarrow e\gamma)$. Concerning the amount of LFV inducing the $\mu \rightarrow e\gamma$ transitions, one finds that, similar

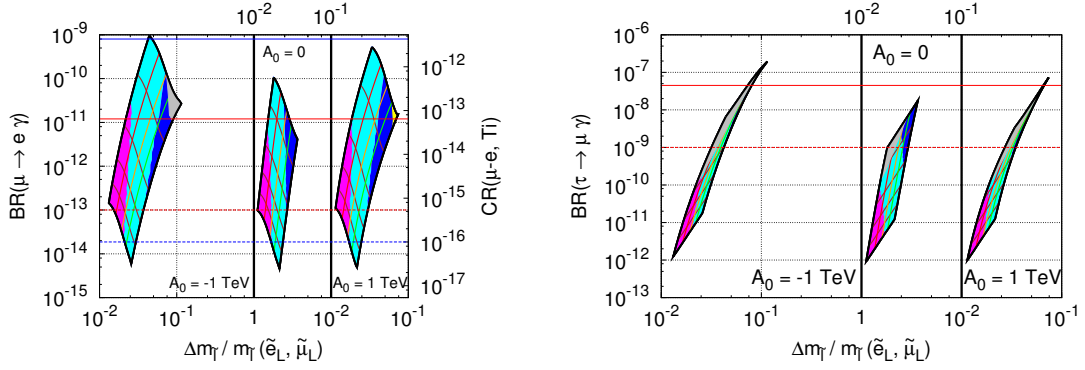


Figure 7. Non-degenerate triplet masses: $\text{BR}(\mu \rightarrow e\gamma)$ and $\text{BR}(\tau \rightarrow \mu\gamma)$ as a function of the $\tilde{e}_L - \tilde{\mu}_L$ slepton mass difference (normalised to an average slepton mass), corresponding to the left- and right-hand side panels. Same scan as leading to figure 6, except that now $M_{N_{1,3}}$ are fixed, with varying M_{N_2} : $M_{N_1} = 10^{13} \text{ GeV} \lesssim M_{N_2} \lesssim 9 \times 10^{14} \text{ GeV} = M_{N_3}$. Same line and colour code as in figure 6, the only exception being that the inset “vertical” isolines for M_{N_2} decrease from left to right.

to what occurs in the degenerate case, the largest BRs are associated with M_{N_2} close to its maximal allowed value (i.e. $\sim M_{N_3}$, leading to degenerate heavy and next-to-heavy triplets) and minimal values of $M_{1/2}$. While the latter leads to a lighter spectrum, the former allows to enhance the $(Y^{\nu\dagger}LY^\nu)_{21}$ contributions proportional to M_{N_2} , which are not suppressed by the smallness of θ_{13} . However, it is important to notice that the same does not occur regarding $\text{BR}(\tau \rightarrow \mu\gamma)$, which is maximal for both minimal values of $M_{1/2}$ and M_{N_2} (now degenerate with the lightest triplet). For fixed values of $M_{N_{1,3}}$, while the flavour violating entries responsible for $\mu \rightarrow e\gamma$ transitions and other decays involving the first lepton family (i.e. $(\Delta m_L^2)_{12}$ and $(\Delta m_L^2)_{13}$) increase with increasing M_{N_2} , $(\Delta m_L^2)_{23}$ - which induces $\text{BR}(\tau \rightarrow \mu\gamma)$ - remains approximately constant: in fact it actually decreases by a small factor, since the contributions proportional to M_{N_2} have the opposite sign of those associated to M_{N_3} .

For completeness, and before concluding the discussion of LFV in the case of hierarchical heavy triplets, we present on the left panel of figure 8 the corresponding average squark masses as a function of the next-to-lightest triplet mass, for different values of m_0 (similar to the analysis presented in figure 2 for the case of a degenerate triplet spectrum). As can be directly verified, squarks are also considerably heavy in the hierarchical triplet case, albeit not as heavy as for the degenerate case.

On the right panel of figure 8 we reconstitute the same analysis of figure 5, evaluating the ratio of slepton mass differences as a function of the next-to-lightest triplet mass. Likewise, one verifies that the ratio of slepton mass splittings is in good agreement with the analytical relation of eq. (3.4). When compared to the degenerate triplet case investigated in figure 5, the shape of the curve is somewhat different, an effect due to having fixed the values of the heaviest and lightest triplet.

A final comment is still in order concerning the impact of a different mass hierarchy for the light neutrinos, ν_i . Considering an inverted hierarchy for ν_i would lead to scenarios

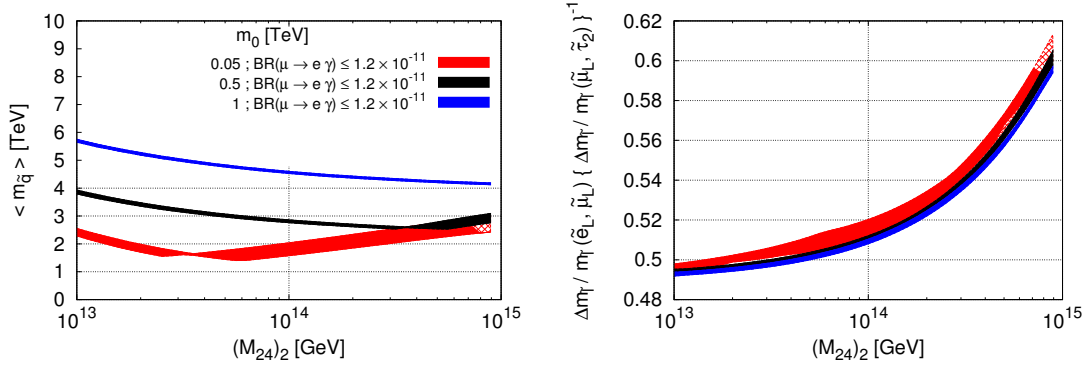


Figure 8. On the left, average squark mass range (in TeV) as a function of the next-to-lightest triplet mass $(M_{24})_2$ (in GeV). On the right, ratio of slepton mass differences, $\Delta m_{\tilde{\ell}}(\tilde{e}_L, \tilde{\mu}_L) / \Delta m_{\tilde{\ell}}(\tilde{\mu}_L, \tilde{\tau}_2)$ (normalised to the corresponding average slepton mass), as a function of the next-to-lightest triplet mass $(M_{24})_2$ (in GeV). In both cases, $\tan\beta = 10$, $A_0 = \{-1, 0, 1\}$ TeV and $\theta_{13} = 0.1^\circ$, and we consider different values of m_0 : 50 GeV (blue), 500 GeV (black) and 1 TeV (red), gridded regions corresponding to cases where one has a charged LSP. Same scan as leading to figure 5, but except that now $M_{N_{1,3}}$ are fixed, with varying M_{N_2} (represented by $(M_{24})_2$): $M_{N_1} = 10^{13}$ GeV $\lesssim M_{N_2} \lesssim 9 \times 10^{14}$ GeV $= M_{N_3}$.

of LFV that are qualitatively similar to those explored here, in particular to the case of degenerate triplet masses (with a normal hierarchy for ν_i).

Finally, and to conclude our numerical study, we have considered deviations from the $R = 1$ limit, i.e., allowing for additional mixings in the seesaw mediators. Non-vanishing angles θ_i lead to larger Y_{ij}^ν , with implications for LFV observables: as expected (and aside from eventual accidental cancelations), there is a large enhancement of the contributions to low-energy LFV observables, as well as an increase of the mass splittings. More concretely, this would displace the cyan regions in figures 6 and 7 towards larger values of $\text{BR}(\mu \rightarrow e\gamma)$ - potentially excluded by current bounds - and towards slightly larger $\tilde{e}_L - \tilde{\mu}_L$ mass differences. Notice that when compared to the type I SUSY seesaw, the effects of $R \neq 1$ are somewhat less important, since due to the much narrower interval of the seesaw scale (which is also heavier), perturbativity of Y^ν effectively constraints the values of θ_i . Concerning the impact of these variations on the SUSY spectrum (RGE induced), we have verified that deviations from $R = 1$ have no effect on the gaugino and squark spectra.

To summarise, let us re-emphasise that should the $\chi_2^0 \rightarrow \chi_1^0 \ell\ell$ decay chain be reconstructed at the LHC (even if challenging due to a typically heavy SUSY spectrum), a type III SUSY seesaw would be manifest in both low- and high-energy LFV observables: in particular, $\text{BR}(\mu \rightarrow e\gamma)$ is likely to be within MEG reach in the near future, while $\Delta m_{\tilde{\ell}}/m_{\tilde{\ell}}(\tilde{e}_L, \tilde{\mu}_L)$ of the order of % render the slepton mass splittings potentially identifiable at the LHC (provided there are enough events allowing the reconstruction of the χ_2^0 decay chain).

5 Conclusions

Although it is a very appealing hypothesis to explain the origin of neutrino masses and mixings, the seesaw mechanism is in general very hard to probe directly. When embedded into a larger framework (as for instance SUSY models), where new states are active between the seesaw scale and the electroweak one, the seesaw mechanism can give rise to many distinct signatures, depending on the nature of the mediators: scalar or fermionic (gauge singlets or triplets). In this study we considered a supersymmetric type III seesaw where, in order to preserve gauge coupling unification, the additional states are embedded into complete $SU(5)$ representations. The many experimental constraints (LEP, LHC, low-energy experiments) strongly reduce the available parameter space of the model, so that one expects very characteristic signals (SUSY spectrum and charged LFV, both at low-energies and at the LHC), which offer the possibility of falsifying the model. Using the correlation between the different LFV observables (inherent from the assumption that the seesaw provides the only source of flavour violation in the model), we have focused our analysis on the interplay between low-energy radiative decays (e.g. $\mu \rightarrow e\gamma$) and potential LFV signatures appearing in association with the $\chi_2^0 \rightarrow \tilde{\ell}\ell$ cascade decays at the LHC, such as flavoured slepton mass splittings, $\Delta m_{\tilde{\ell}}/m_{\tilde{\ell}} (\tilde{e}_L, \tilde{\mu}_L)$.

Firstly, requiring that the spectrum allows for the reconstruction of slepton masses from the χ_2^0 cascade decay chains (and assuming a χ_1^0 LSP), the type III SUSY seesaw leads to scenarios where a heavy SUSY spectrum (e.g. $m_{\tilde{q}} \sim 2\text{ TeV}$) is in general favoured. Although viable dark matter scenarios are in general very hard to accommodate in the type III seesaw, we have nevertheless verified that one can still find small regions in the parameter space where the χ_1^0 has the correct relic density. Such scenarios typically arise in association with the low m_0 regime. Concerning dark matter, it is important to recall that other candidates might be present and have a relic density in agreement with WMAP bounds, as could be the case for gravitinos. However, this issue clearly lies beyond the scope of the present work.

Assuming that a type III seesaw is indeed the only source of LFV, and given the extremely constrained parameter space, one finds that the slepton mass splittings $\tilde{e}_L - \tilde{\mu}_L$ will always lie around the % level. A hierarchical fermionic triplet spectrum further boosts the expected mass splittings: one is led to a regime where, even in the conservative limit of $R = 1$, one has $1\% \lesssim \Delta m_{\tilde{\ell}}/m_{\tilde{\ell}} (\tilde{e}_L, \tilde{\mu}_L) \lesssim 5\%$, in agreement with current bounds on charged LFV. Furthermore, these mass splittings correspond to values of $\text{BR}(\mu \rightarrow e\gamma)$ well within the expected sensitivity of MEG (or, in very limiting cases, within PRISM/PRIME sensitivity for $\text{CR}(\mu - e, \text{Ti})$).

In the more general case of an increased mixing involving the triplet sector (i.e. $R \neq 1$), there is an enhancement of the contributions to low-energy LFV observables, as well as a small increase in the slepton mass splittings, without further impact on the remaining SUSY spectrum.

Unlike what occurs for a type I SUSY seesaw, the very constrained range for the type III seesaw scale strongly tightens the predictions for LFV: the expected flavoured mass splittings $\tilde{e}_L - \tilde{\mu}_L$ are potentially within the sensitivity range of the LHC, while at the same time low-energy scale LFV must unavoidably lie within the present and future

sensitivity of either MEG or PRISM/PRIME (observation of a $\tau \rightarrow \mu\gamma$ signal at SuperB will be much more challenging). If supersymmetry is discovered at the LHC, and a type III seesaw is at the origin of flavour mixing in the lepton sector, then this model can be easily falsified in the near future.

Acknowledgments

This work has been done partly under the ANR project CPV-LFV-LHC NT09-508531. The work of A. J. R. F. has been supported by *Fundação para a Ciência e a Tecnologia* through the fellowship SFRH/BD/64666/2009. A. J. R. F. and J. C. R. also acknowledge the financial support from the EU Network grant UNILHC PITN-GA-2009-237920 and from *Fundação para a Ciência e a Tecnologia* grants CFTP-FCT UNIT 777, CERN/FP/83503/2008 and PTDC/FIS/102120/2008.

Open Access. This article is distributed under the terms of the Creative Commons Attribution Noncommercial License which permits any noncommercial use, distribution, and reproduction in any medium, provided the original author(s) and source are credited.

References

- [1] P. Minkowski, $\mu \rightarrow e\gamma$ at a rate of one out of 1-billion muon decays?, *Phys. Lett. B* **67** (1977) 421 [[SPIRES](#)].
- [2] M. Gell-Mann, P. Ramond and R. Slansky, *Complex spinors and unified theories*, in *Supergravity*, P. Van. Nieuwenhuizen and D. Z. Freedman eds., North-Holland, Amsterdam The Netherlands (1979).
- [3] T. Yanagida, *Horizontal gauge symmetry and masses of neutrinos*, in the proceedings of the *Workshop on the unified theory and the baryon number in the universe*, February 13–14, KEK, Tsukuba, Japan (1979).
- [4] S.L. Glashow, *The future of elementary particle physics*, in *Quarks and leptons*, M. Lévy et al. eds., Plenum Press, New York, U.S.A. (1980) [*NATO Adv. Study Inst. Ser. B Phys.* **59** (1980) 687].
- [5] R.N. Mohapatra and G. Senjanović, *Neutrino mass and spontaneous parity nonconservation*, *Phys. Rev. Lett.* **44** (1980) 912 [[SPIRES](#)].
- [6] R. Barbieri, D.V. Nanopoulos, G. Morchio and F. Strocchi, *Neutrino masses in grand unified theories*, *Phys. Lett. B* **90** (1980) 91 [[SPIRES](#)].
- [7] R.E. Marshak and R.N. Mohapatra, *Selection rules for baryon number nonconservation in gauge models*, invited talk given at *Orbis Scientiae*, January 14–17, Coral Gables, U.S.A. (1980) [[SPIRES](#)].
- [8] T.P. Cheng and L.-F. Li, *Neutrino masses, mixings and oscillations in $SU(2) \times U(1)$ models of electroweak interactions*, *Phys. Rev. D* **22** (1980) 2860 [[SPIRES](#)].
- [9] M. Magg and C. Wetterich, *Neutrino mass problem and gauge hierarchy*, *Phys. Lett. B* **94** (1980) 61 [[SPIRES](#)].
- [10] G. Lazarides, Q. Shafi and C. Wetterich, *Proton lifetime and fermion masses in an $SO(10)$ model*, *Nucl. Phys. B* **181** (1981) 287 [[SPIRES](#)].

- [11] J. Schechter and J.W.F. Valle, *Neutrino masses in $SU(2) \times U(1)$ theories*, *Phys. Rev. D* **22** (1980) 2227 [SPIRES].
- [12] R.N. Mohapatra and G. Senjanović, *Neutrino masses and mixings in gauge models with spontaneous parity violation*, *Phys. Rev. D* **23** (1981) 165 [SPIRES].
- [13] E. Ma, *Pathways to naturally small neutrino masses*, *Phys. Rev. Lett.* **81** (1998) 1171 [hep-ph/9805219] [SPIRES].
- [14] R. Foot, H. Lew, X.G. He and G.C. Joshi, *Seesaw neutrino masses induced by a triplet of leptons*, *Z. Phys. C* **44** (1989) 441 [SPIRES].
- [15] G. Jungman, M. Kamionkowski and K. Griest, *Supersymmetric dark matter*, *Phys. Rept.* **267** (1996) 195 [hep-ph/9506380] [SPIRES].
- [16] G. Bertone, D. Hooper and J. Silk, *Particle dark matter: evidence, candidates and constraints*, *Phys. Rept.* **405** (2005) 279 [hep-ph/0404175] [SPIRES].
- [17] D. Larson et al., *Seven-year Wilkinson Microwave Anisotropy Probe (WMAP) observations: power spectra and WMAP-derived parameters*, *Astrophys. J. Suppl.* **192** (2011) 16 [arXiv:1001.4635] [SPIRES].
- [18] J. Hisano, T. Moroi, K. Tobe and M. Yamaguchi, *Lepton-flavor violation via right-handed neutrino Yukawa couplings in supersymmetric standard model*, *Phys. Rev. D* **53** (1996) 2442 [hep-ph/9510309] [SPIRES].
- [19] J. Hisano, T. Moroi, K. Tobe, M. Yamaguchi and T. Yanagida, *Lepton flavor violation in the supersymmetric standard model with seesaw induced neutrino masses*, *Phys. Lett. B* **357** (1995) 579 [hep-ph/9501407] [SPIRES].
- [20] J. Hisano and D. Nomura, *Solar and atmospheric neutrino oscillations and lepton flavor violation in supersymmetric models with the right-handed neutrinos*, *Phys. Rev. D* **59** (1999) 116005 [hep-ph/9810479] [SPIRES].
- [21] W. Buchmüller, D. Delepine and F. Vissani, *Neutrino mixing and the pattern of supersymmetry breaking*, *Phys. Lett. B* **459** (1999) 171 [hep-ph/9904219] [SPIRES].
- [22] Y. Kuno and Y. Okada, *Muon decay and physics beyond the standard model*, *Rev. Mod. Phys.* **73** (2001) 151 [hep-ph/9909265] [SPIRES].
- [23] J.A. Casas and A. Ibarra, *Oscillating neutrinos and $\mu \rightarrow e\gamma$* , *Nucl. Phys. B* **618** (2001) 171 [hep-ph/0103065] [SPIRES].
- [24] S. Lavignac, I. Masina and C.A. Savoy, *$\tau \rightarrow \mu\gamma$ and $\mu \rightarrow e\gamma$ as probes of neutrino mass models*, *Phys. Lett. B* **520** (2001) 269 [hep-ph/0106245] [SPIRES].
- [25] X.-J. Bi and Y.-B. Dai, *Lepton flavor violation and its constraints on the neutrino mass models*, *Phys. Rev. D* **66** (2002) 076006 [hep-ph/0112077] [SPIRES].
- [26] J.R. Ellis, J. Hisano, M. Raidal and Y. Shimizu, *A new parametrization of the seesaw mechanism and applications in supersymmetric models*, *Phys. Rev. D* **66** (2002) 115013 [hep-ph/0206110] [SPIRES].
- [27] F. Deppisch, H. Pas, A. Redelbach, R. Ruckl and Y. Shimizu, *Probing the Majorana mass scale of right-handed neutrinos in $mSUGRA$* , *Eur. Phys. J. C* **28** (2003) 365 [hep-ph/0206122] [SPIRES].
- [28] T. Fukuyama, T. Kikuchi and N. Okada, *Lepton flavor violating processes and muon $g - 2$ in minimal supersymmetric $SO(10)$ model*, *Phys. Rev. D* **68** (2003) 033012 [hep-ph/0304190] [SPIRES].

- [29] A. Brignole and A. Rossi, *Anatomy and phenomenology of $\mu\tau$ lepton flavour violation in the MSSM*, *Nucl. Phys. B* **701** (2004) 3 [[hep-ph/0404211](#)] [[SPIRES](#)].
- [30] A. Masiero, S.K. Vempati and O. Vives, *Massive neutrinos and flavour violation*, *New J. Phys.* **6** (2004) 202 [[hep-ph/0407325](#)] [[SPIRES](#)].
- [31] T. Fukuyama, A. Ilakovac and T. Kikuchi, *Lepton flavour violating leptonic/semileptonic decays of charged leptons in the minimal supersymmetric standard model*, *Eur. Phys. J. C* **56** (2008) 125 [[hep-ph/0506295](#)] [[SPIRES](#)].
- [32] S.T. Petcov, W. Rodejohann, T. Shindou and Y. Takanishi, *The see-saw mechanism, neutrino Yukawa couplings, LFV decays $l(i) \rightarrow l(j) + \gamma$ and leptogenesis*, *Nucl. Phys. B* **739** (2006) 208 [[hep-ph/0510404](#)] [[SPIRES](#)].
- [33] E. Arganda and M.J. Herrero, *Testing supersymmetry with lepton flavor violating τ and μ decays*, *Phys. Rev. D* **73** (2006) 055003 [[hep-ph/0510405](#)] [[SPIRES](#)].
- [34] F. Deppisch, H. Pas, A. Redelbach and R. Ruckl, *Constraints on SUSY seesaw parameters from leptogenesis and lepton flavor violation*, *Phys. Rev. D* **73** (2006) 033004 [[hep-ph/0511062](#)] [[SPIRES](#)].
- [35] C.E. Yaguna, *Constraining mSUGRA parameters with $\mu \rightarrow e\gamma$ and μ -e conversion in nuclei*, *Int. J. Mod. Phys. A* **21** (2006) 1283 [[hep-ph/0502014](#)] [[SPIRES](#)].
- [36] L. Calibbi, A. Faccia, A. Masiero and S.K. Vempati, *Lepton flavour violation from SUSY-GUTs: Where do we stand for MEG, PRISM/PRIME and a super flavour factory*, *Phys. Rev. D* **74** (2006) 116002 [[hep-ph/0605139](#)] [[SPIRES](#)].
- [37] S. Antusch, E. Arganda, M.J. Herrero and A.M. Teixeira, *Impact of θ_{13} on lepton flavour violating processes within SUSY seesaw*, *JHEP* **11** (2006) 090 [[hep-ph/0607263](#)] [[SPIRES](#)].
- [38] M. Hirsch, J.W.F. Valle, W. Porod, J.C. Romao and A. Villanova del Moral, *Probing minimal supergravity in type-I seesaw with lepton flavour violation at the LHC*, *Phys. Rev. D* **78** (2008) 013006 [[arXiv:0804.4072](#)] [[SPIRES](#)].
- [39] E. Arganda, M.J. Herrero and A.M. Teixeira, *μ -e conversion in nuclei within the CMSSM seesaw: universality versus non-universality*, *JHEP* **10** (2007) 104 [[arXiv:0707.2955](#)] [[SPIRES](#)].
- [40] E. Arganda, M.J. Herrero and J. Portoles, *Lepton flavour violating semileptonic tau decays in constrained MSSM-seesaw scenarios*, *JHEP* **06** (2008) 079 [[arXiv:0803.2039](#)] [[SPIRES](#)].
- [41] N. Arkani-Hamed, H.-C. Cheng, J.L. Feng and L.J. Hall, *Probing lepton flavor violation at future colliders*, *Phys. Rev. Lett.* **77** (1996) 1937 [[hep-ph/9603431](#)] [[SPIRES](#)].
- [42] I. Hinchliffe and F.E. Paige, *Lepton flavor violation at the LHC*, *Phys. Rev. D* **63** (2001) 115006 [[hep-ph/0010086](#)] [[SPIRES](#)].
- [43] D.F. Carvalho, J.R. Ellis, M.E. Gomez, S. Lola and J.C. Romao, *τ flavour violation in sparticle decays at the LHC*, *Phys. Lett. B* **618** (2005) 162 [[hep-ph/0206148](#)] [[SPIRES](#)].
- [44] E. Carquin, J. Ellis, M.E. Gomez, S. Lola and J. Rodriguez-Quintero, *Search for τ flavour violation at the LHC*, *JHEP* **05** (2009) 026 [[arXiv:0812.4243](#)] [[SPIRES](#)].
- [45] F.E. Paige, *Determining SUSY particle masses at LHC*, in the proceedings of the DPF/DPB summer study on new directions for high-energy physics (Snowmass 96), June 25–July 12, Snowmass, Colorado, U.S.A. (1996), [[hep-ph/9609373](#)] [[SPIRES](#)].
- [46] I. Hinchliffe, F.E. Paige, M.D. Shapiro, J. Soderqvist and W. Yao, *Precision SUSY measurements at CERN LHC*, *Phys. Rev. D* **55** (1997) 5520 [[hep-ph/9610544](#)] [[SPIRES](#)].

- [47] H. Bachacou, I. Hinchliffe and F.E. Paige, *Measurements of masses in SUGRA models at CERN LHC*, *Phys. Rev. D* **62** (2000) 015009 [[hep-ph/9907518](#)] [[SPIRES](#)].
- [48] CMS collaboration, G.L. Bayatian et al., *CMS technical design report, volume II: physics performance*, *J. Phys. G* **34** (2007) 995 [[SPIRES](#)].
- [49] ATLAS v collaboration, W.W. Armstrong et al., *ATLAS: technical proposal for a general-purpose pp experiment at the Large Hadron Collider at CERN*, *CERN-LHCC-94-43* (1994) [[SPIRES](#)].
- [50] THE ATLAS collaboration, G. Aad et al., *Expected performance of the ATLAS experiment — Detector, trigger and physics*, [arXiv:0901.0512](#) [[SPIRES](#)].
- [51] A. Abada, A.J.R. Figueiredo, J.C. Romao and A.M. Teixeira, *Interplay of LFV and slepton mass splittings at the LHC as a probe of the SUSY seesaw*, *JHEP* **10** (2010) 104 [[arXiv:1007.4833](#)] [[SPIRES](#)].
- [52] R. Foot, H. Lew, X.G. He and G.C. Joshi, *Seesaw neutrino masses induced by a triplet of leptons*, *Z. Phys. C* **44** (1989) 441 [[SPIRES](#)].
- [53] M.R. Buckley and H. Murayama, *How can we test seesaw experimentally?*, *Phys. Rev. Lett.* **97** (2006) 231801 [[hep-ph/0606088](#)] [[SPIRES](#)].
- [54] B. Bajc and G. Senjanović, *Seesaw at LHC*, *JHEP* **08** (2007) 014 [[hep-ph/0612029](#)] [[SPIRES](#)].
- [55] C. Biggio and L. Calibbi, *Phenomenology of SUSY SU(5) with type-I+III seesaw*, *JHEP* **10** (2010) 037 [[arXiv:1007.3750](#)] [[SPIRES](#)].
- [56] J.N. Esteves, J.C. Romao, M. Hirsch, F. Staub and W. Porod, *Supersymmetric type-III seesaw: lepton flavour violating decays and dark matter*, *Phys. Rev. D* **83** (2011) 013003 [[arXiv:1010.6000](#)] [[SPIRES](#)].
- [57] I. Hinchliffe and F.E. Paige, *Measurements in SUGRA models with large $\tan\beta$ at LHC*, *Phys. Rev. D* **61** (2000) 095011 [[hep-ph/9907519](#)] [[SPIRES](#)].
- [58] H. Bachacou, I. Hinchliffe and F.E. Paige, *Measurements of masses in SUGRA models at CERN LHC*, *Phys. Rev. D* **62** (2000) 015009 [[hep-ph/9907518](#)] [[SPIRES](#)].
- [59] B.C. Allanach, J.P. Conlon and C.G. Lester, *Measuring smuon-selectron mass splitting at the CERN LHC and patterns of supersymmetry breaking*, *Phys. Rev. D* **77** (2008) 076006 [[arXiv:0801.3666](#)] [[SPIRES](#)].
- [60] ATLAS collaboration, G. Aad et al., *Search for supersymmetry using final states with one lepton, jets and missing transverse momentum with the ATLAS detector in $\sqrt{s} = 7$ TeV pp*, *Phys. Rev. Lett.* **106** (2011) 131802 [[arXiv:1102.2357](#)] [[SPIRES](#)].
- [61] CMS collaboration, V. Khachatryan et al., *Search for supersymmetry in pp collisions at 7 TeV in events with jets and missing transverse energy*, *Phys. Lett. B* **698** (2011) 196 [[arXiv:1101.1628](#)] [[SPIRES](#)].
- [62] A.J. Buras, L. Calibbi and P. Paradisi, *Slepton mass-splittings as a signal of LFV at the LHC*, *JHEP* **06** (2010) 042 [[arXiv:0912.1309](#)] [[SPIRES](#)].
- [63] M. Raidal et al., *Flavour physics of leptons and dipole moments*, *Eur. Phys. J. C* **57** (2008) 13 [[arXiv:0801.1826](#)] [[SPIRES](#)].
- [64] W. Porod, *SPheno, a program for calculating supersymmetric spectra, SUSY particle decays and SUSY particle production at e^+e^- colliders*, *Comput. Phys. Commun.* **153** (2003) 275 [[hep-ph/0301101](#)] [[SPIRES](#)].
- [65] F. Staub, *SARAH*, *Comput. Phys. Commun.* **181** (2010) 1077 [[arXiv:0806.0538](#)] [[SPIRES](#)].

- [66] G. Bélanger, F. Boudjema, A. Pukhov and A. Semenov, *Dark matter direct detection rate in a generic model with MicrOMEGAs2.1*, *Comput. Phys. Commun.* **180** (2009) 747 [[arXiv:0803.2360](#)] [[SPIRES](#)].
- [67] M.C. Gonzalez-Garcia, M. Maltoni and J. Salvado, *Updated global fit to three neutrino mixing: status of the hints of $\theta_{13} > 0$* , *JHEP* **04** (2010) 056 [[arXiv:1001.4524](#)] [[SPIRES](#)].
- [68] PARTICLE DATA GROUP collaboration, K. Nakamura et al., *Review of particle physics*, *J. Phys. G* **37** (2010) 075021 [[SPIRES](#)].
- [69] MEG collaboration, O.A. Kiselev, *Positron spectrometer of MEG experiment at PSI*, *Nucl. Instrum. Meth. A* **604** (2009) 304 [[SPIRES](#)].
- [70] BELLE collaboration, K. Hayasaka et al., *New search for $\tau \rightarrow \mu\gamma$ and $\tau \rightarrow e\gamma$ decays at Belle*, *Phys. Lett. B* **666** (2008) 16 [[arXiv:0705.0650](#)] [[SPIRES](#)].
- [71] SUPERB collaboration, M. Bona et al., *SuperB: a high-luminosity asymmetric e^+e^- super flavor factory. Conceptual design report*, [arXiv:0709.0451](#) [[SPIRES](#)].
- [72] D. Glenzinski, *The Mu2e experiment at Fermilab*, *AIP Conf. Proc.* **1222** (2010) 383 [[SPIRES](#)].
- [73] COMET collaboration, Y.G. Cui et al., *Conceptual design report for experimental search for lepton flavor violating μ^-e^- conversion at sensitivity of 10^{-16} with a slow-extracted bunched proton beam (COMET)*, KEK-2009-10 [[SPIRES](#)].
- [74] LEP WORKING GROUP FOR HIGGS BOSON SEARCHES collaboration, R. Barate et al., *Search for the standard model Higgs boson at LEP*, *Phys. Lett. B* **565** (2003) 61 [[hep-ex/0306033](#)] [[SPIRES](#)].
- [75] P. Totaro, *High mass SM Higgs*, talk given at the XLVIth Rencontres de Moriond. *Electroweak interactions and unified theories*, March 13–20, La Thuile, France (2011).
- [76] K. Petridis, *Search for low mass Higgs boson at the Tevatron*, talk given at the XLVIth Rencontres de Moriond. *Electroweak interactions and unified theories*, March 13–20, La Thuile, France (2011).